# $^4$He adsorption on a single graphene sheet: Path-integral Monte Carlo study

Yongkyung Kwon[1] and David M. Ceperley[2]
[1]*Division of Quantum Phases and Devices, School of Physics, Konkuk University, Seoul 143-701, Korea*
[2]*Department of Physics, University of Illinois at Urbana-Champaign, Urbana, Illinois 61801, USA*
(Received 14 November 2011; published 4 June 2012)

We have performed path-integral Monte Carlo calculations to study $^4$He adsorption on a single graphene sheet. The $^4$He-substrate interaction was assumed to be a pairwise sum of the helium-carbon potentials constructed by Carlos and Cole to fit helium scattering data from a graphite surface. We employed both an anisotropic 6-12 Lennard-Jones potential and a spherical 6-12 potential. For both potentials, the first $^4$He layer has the $C_{1/3}$ commensurate structure at a surface density of 0.0636 Å$^{-2}$. Vacancy states created in the $C_{1/3}$ commensurate solid, however, behave differently depending on the $^4$He-substrate interaction: a cluster of localized vacancies are formed with the fully anisotropic 6-12 pair potentials while mobile vacancies are found to induce finite superfluid fractions with the substrate potential based on only the isotropic parts of the inter-atomic pair potentials. For the second helium layer we find that exchange among $^4$He adatoms results in quantum melting of a $C_{7/12}$ commensurate structure, which is registered to a first-layer triangular solid. The possible stabilization of this commensurate structure with the addition of $^3$He impurities is discussed.

DOI: 10.1103/PhysRevB.85.224501 PACS number(s): 67.25.bh, 67.80.dm, 67.80.bd, 67.25.dj

## I. INTRODUCTION

Graphene, a single layer of carbon atoms densely packed in a honeycomb crystal lattice, has attracted much attention as a novel material for nano-electronic devices because of its unique electronic properties. It is also one of the strongest materials ever found, leading to active exploration for possible nano-electromechanical systems applications such as pressure sensors and resonators. A recently created balloon-like graphene membrane was found to be ultrastrong and impermeable to even the lightest inert gas atoms, i.e., helium atoms.[1]

Graphite is a stack of graphene sheets with an interplanar spacing of 3.35 Å. Due to strong binding of helium atoms on its surface, multiple distinct layers of $^4$He atoms are found on graphite.[2] These helium adlayers on graphite exhibit very rich structural phase diagrams, as a result of the interplay between the helium-substrate interaction and helium-helium interactions. It is well established that the $^4$He monolayer on graphite shows the $C_{1/3}$ commensurate structure at a surface density of 0.0636 Å$^{-2}$ and goes through domain wall phases at higher densities before crystallizing into an incommensurate triangular solid.[3,4] Torsional oscillator experiments of Crowell and Reppy first revealed re-entrant superfluid responses of the second and third helium layers on graphite,[5,6] which prompted an early speculation of possible two-dimensional supersolidity. However, even after several decades of intensive experimental and theoretical investigation, the microscopic structures and dynamics of these layers are not fully understood as a function of helium coverage. For example, the existence of a stable commensurate solid phase in the second $^4$He layer on graphite is still under debate. Based on their path-integral Monte Carlo (PIMC) calculations, Pierce and Manousakis predicted a 4/7 commensurate solid phase above a frozen first-layer triangular solid.[7,8] But more recent PIMC calculations of Corboz *et al.*, including the full incorporation of zero-point motions of the first-layer $^4$He atoms, did not find this structure to be stable.[9]

Gordillo and Boronat recently studied different quantum phases of a monolayer of $^4$He adsorption on a single graphene sheet with the diffusion Monte Carlo (DMC) method.[10] Noting very small energy differences between a low-density liquid state and a $C_{1/3}$ commensurate solid, they concluded that a liquid phase could be realized, at least as a metastable state at low helium coverages. In a more recent paper, Gordillo *et al.* reported that the $C_{1/3}$ commensurate structure of $^4$He atoms on a graphene surface could support mobile vacancy states and exhibit two-dimensional supersolidity.[11]

In this paper, we use the PIMC method to investigate the structural and superfluid properties of the first two helium layers adsorbed on the surface of a single graphene sheet. We find that the low-temperature phases of a helium monolayer, especially at low coverages, depend critically on the assumed substrate potential and that a second-layer commensurate structure is disrupted by quantum exchange among $^4$He adatoms.

## II. METHODOLOGY

In our calculations, the helium-graphene interaction $V_{\rm subs}(\vec{r})$ is assumed to be a sum of pair potentials between the carbon atoms and a $^4$He atom:

$$V_{\rm subs}(\vec{r}) = \sum_i V_{\rm He-C}(\vec{r} - \vec{r}_i), \tag{1}$$

where $\vec{r}_i$ represents the position of a carbon atom in the honeycomb structure of graphene. Some years ago Carlos and Cole proposed different empirical helium-carbon pair potentials to fit helium scattering from graphite surfaces.[12] Among them we employ the anisotropic 6-12 Lennard-Jones (LJ) $^4$He-C pair potentials. This approach of modeling the $^4$He-substrate potential with the $^4$He-C pair potentials has been widely used for the study of helium adsorption on the surface of a carbon isomer such as a graphite,[7,9,13] a nanotube,[14–16] and a fullerene molecule.[17–19] We here use the full sum of the anisotropic interatomic pair potentials in Eq. (1) for the $^4$He-graphene interaction while helium corrugations were accounted for by using only a few terms in the Fourier

 

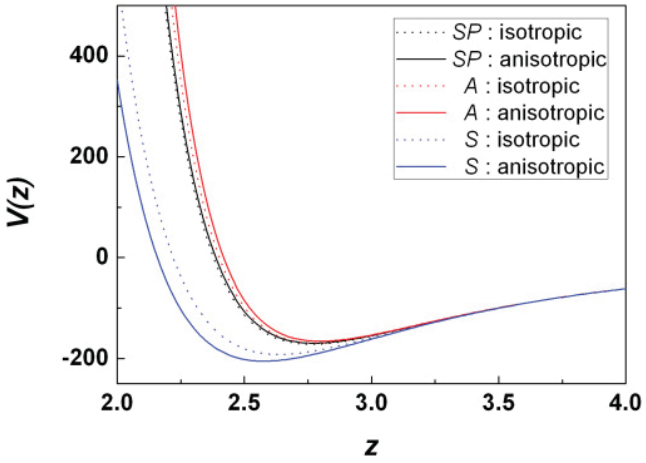


FIG. 1. (Color online) $^4$He-graphene potential energy (in K) along three different symmetry directions as a function of the distance $z$ (in Å) from the graphene surface. The solid lines show the helium-substrate potential made of the fully anisotropic LJ pair potentials and the dotted lines show the interaction potential described by the sum of the isotropic LJ pair potentials. $S$ ($A$) represents the sixfold (threefold) symmetry direction above a hexagon center (a carbon atom) on the graphene surface while $SP$ corresponds to the direction of a saddle point located above the midpoint of a carbon-carbon bond.

expansion of the substrate potential in most of previous theoretical studies of helium adlayers on graphite. On the other hand, Gordillo *et al*. used the $^4$He-graphene potential described by the sum of only the isotropic parts of the LJ pair potentials in their DMC calculations.[10,11] Figure 1 shows the $^4$He-graphene potential energies along three different symmetry directions as a function of the distance from the graphene surface. One can see that the substrate potential based only on the isotropic parts of the pair potentials has significantly less corrugation along the planar directions compared to the complete pair potentials. The leading corrugation amplitude in the $^4$He-graphene potential was estimated in Ref. 20 to decrease by about 33% if only the isotropic parts of the LJ pair potentials are used. This reduced corrugation will affect the low-temperature properties of the $^4$He adlayers, especially of the first layer, as discussed below.

In the discrete path-integral representation, the thermal density matrix at a low temperature $T$ is written as a convolution of $M$ high-temperature density matrices with a time step $\tau = (Mk_BT)^{-1}$. The multilevel Metropolis algorithm described in Ref. 21 is used to sample permutations among $^4$He atoms as well as their imaginary-time paths. For the high-temperature density matrix, the isotropic part of the $^4$He-C pair potential as well as the $^4$He-$^4$He Aziz potential[22] is used to calculate the exact two-body density matrices[21,23] while the anisotropic part of the $^4$He-C potential is treated in the primitive approximation.[21] This is found to provide an accurate description of both the $^4$He-$^4$He and $^4$He-graphene interactions using an imaginary time step of $\tau^{-1}/k_B = 80$ K. Periodic boundary conditions assuming a fixed rectangular cell are used to minimize finite size effects.

## III. RESULTS

### A. The first layer

Using the two different $^4$He-substrate potentials described in Sec. II, we have performed PIMC calculations for a monolayer of $^4$He atoms adsorbed on a single graphene sheet. Figure 2 shows plots of the two-dimensional helium density distributions at a temperature of $T = 0.31$ K, where the number of $^4$He adatoms varies from (a) $N = 36$ to (d) $N = 33$ per $9 \times 6$ rectangular simulation cell. Here the system size is given as multiples of a rectangular unit cell of the honeycomb lattice, which is denoted by the red dotted lines in the top panel of Fig. 2(a). The $9 \times 6$ simulation cell has dimensions of $22.14 \times 25.56$ Å$^{-2}$. The figure for $N = 36$ (density equals 0.0636 Å$^{-2}$) shows the same $\sqrt{3} \times \sqrt{3}$ registered structure with either substrate potential; one out of three adsorption sites on the honeycomb graphene substrate is occupied by a $^4$He atom. According to the DMC calculation of Gordillo and Boronat,[10] this is energetically the most stable state of the helium monolayer with the lowest energy per $^4$He atom. However, when a few particles are removed from the simulation cell, the resulting density distribution depends on the substrate potential. With the substrate potential based on the isotropic pair potentials, the helium density distributions for a single vacancy ($N = 35$) and for two vacancies ($N = 34$) are seen to maintain the $C_{1/3}$ crystal structure; see the top panels of Figs. 2(b) and 2(c). Because of the hopping of $^4$He atoms from occupied sites to vacant sites, the density is still uniform over the $C_{1/3}$ crystalline lattice sites. However, when three particles are removed from the simulation cell, we find a completely different density distribution of $^4$He atoms. As seen in the top panel of Fig. 2(d), the $C_{1/3}$ crystalline structure disappears and every adsorption site has an equal probability of being occupied. We interpret this as a liquid phase in the periodic potential of the substrate. These structural features are consistent with the DMC results of Gordillo *et al*.,[11] which showed activation of mobile vacancies in the $C_{1/3}$ commensurate solid and the transition from the $C_{1/3}$ solid to a liquid at an areal density of $\sigma_c = 0.058$ Å$^{-2}$ corresponding to about three vacancies in our simulation cell.

On the other hand, when the fully anisotropic $^4$He-C pair potentials are used to describe the substrate potential, we find the formation of localized vacancy states. The density distributions shown in the bottom panels of Figs. 2(b)–2(d) suggest that hopping of a $^4$He atom from an occupied site to a vacant site occurs rarely so that the (path integral) mobilities of these vacancies are small. When more particles are removed from the simulation cell, these localized vacancies are found to cluster; see the bottom panel of Fig. 2(d). One interpretation is that the monolayer is in a mixed phase, i.e., a gas-solid state, as predicted by Pierce and Manousakis[13] at this density on a graphite surface.

The structural dependence of the helium monolayer on the substrate potential described above was also observed in the PIMC calculations for a larger system. Figure 3 shows the peak values of the static structure factor obtained with both $9 \times 6$ and $12 \times 8$ simulation cells, as a function of helium coverage. For all the helium coverages considered here, the structure factor is found to be peaked at reciprocal primitive vectors of the 1/3 commensurate solid, which have a magnitude of

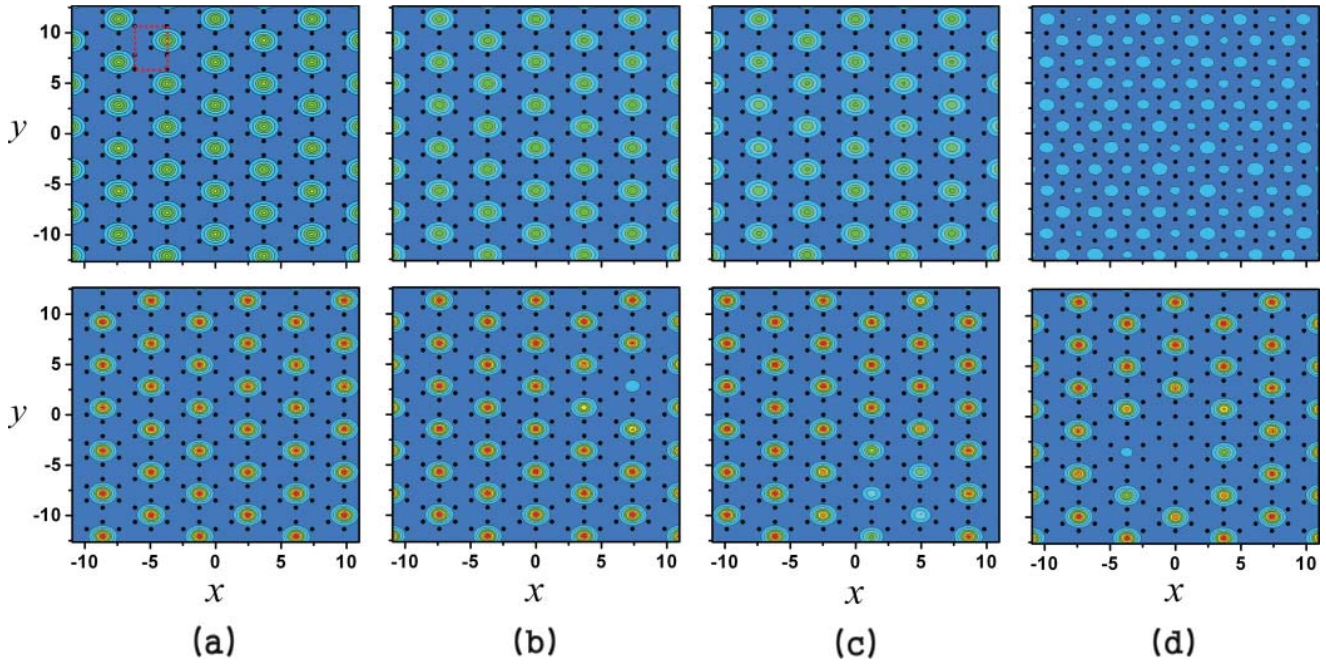


FIG. 2. (Color online) Plots of the two-dimensional helium density on a graphene surface with (a) $N = 36$, (b) $N = 35$, (c) $N = 34$, and (d) $N = 33$ $^4$He adatoms per $9 \times 6$ rectangular simulation cell (red, high density; blue, low density) at $T = 0.31$ K. The black dots represent the positions of the carbon atoms. The unit of length is Å. The top row shows PIMC results obtained with the isotropic LJ $^4$He-C pair potentials while the bottom row represents the results from the anisotropic LJ pair potentials.

1.70 Å$^{-1}$. For the substrate potential based on the anisotropic $^4$He-C pair potentials, the peak values of the structure factor divided by the number of $^4$He atoms change very little as the coverage decreases from the 1/3 commensurate filling of 0.0636 to 0.0477 Å$^{-2}$. This reflects the observation from the bottom row of Fig. 2 that the 1/3 commensurate structure is sustained, at least locally, as the helium coverage decreases below the 1/3 commensurate filling. With the isotropic pair potentials, a big change in the structure factor is observed for coverages between 0.0601 Å$^{-2}$ ($N = 34$ for the $9 \times 6$ cell) and 0.583 Å$^{-2}$ ($N = 33$ for the $9 \times 6$ cell). This confirms the above conclusion that the helium monolayer undergoes structural change from the 1/3 commensurate structure to a liquid state as the helium coverage decreases. The slight difference between the results for the two different system sizes in Fig. 3 says that the structural features described above are not affected by the finite sizes of our systems.

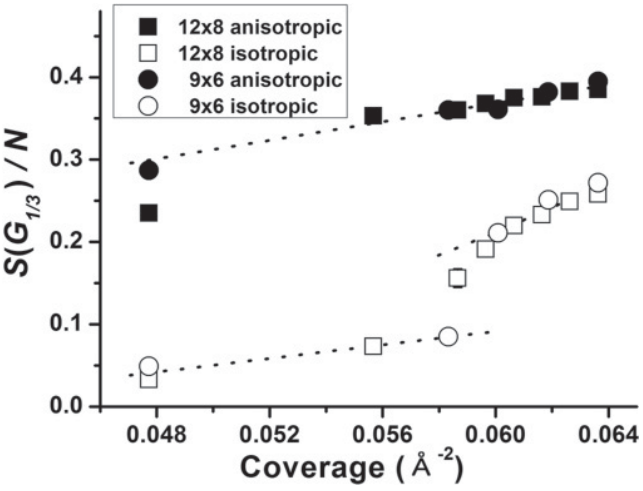


FIG. 3. The peak values of the structure factor divided by the number of $^4$He atoms in the first helium layer on graphene, as a function of helium coverage. The squares (circles) represent the PIMC data for the $12 \times 8$ ($9 \times 6$) simulation cell and the closed (open) symbols denote the results computed with the anisotropic (isotropic) interatomic LJ pair potentials. The dotted lines are just guides for eyes.

We have also found that the helium monolayer shows very different superfluid properties, depending on the choice of the substrate potential. Figure 4 shows the superfluid fraction of the 1/3 commensurate structure for the $9 \times 6$ system.[24] Here $N_v$ is the number of vacancies per simulation cell. No superfluidity (winding paths) was observed for the perfect $C_{1/3}$ crystalline solid (no vacancies), whether we used the anisotropic or the isotropic LJ pair potentials. For the isotropic pair potential, we found a linear dependence of the superfluid fraction on the number of vacancies $N_v$, especially for $N_v \leqslant 2$. This was also observed in the DMC calculations of Gordillo *et al.*[11] The large superfluid fraction for $N_v = 3$ supports the interpretation that it is in a liquid phase as indicated by the homogeneous density in the top panel of Fig. 2(d). These PIMC results are consistent with the DMC results of Gordillo *et al.*, which showed that mobile vacancy states created in the $C_{1/3}$ structure would induce finite superfluid fractions and hence support two-dimensional supersolidity. However, the $C_{1/3}$ solids with localized vacancies, which occur with the anisotropic $^4$He-C pair potentials, do not show superfluid response. We conclude that both structural and superfluid

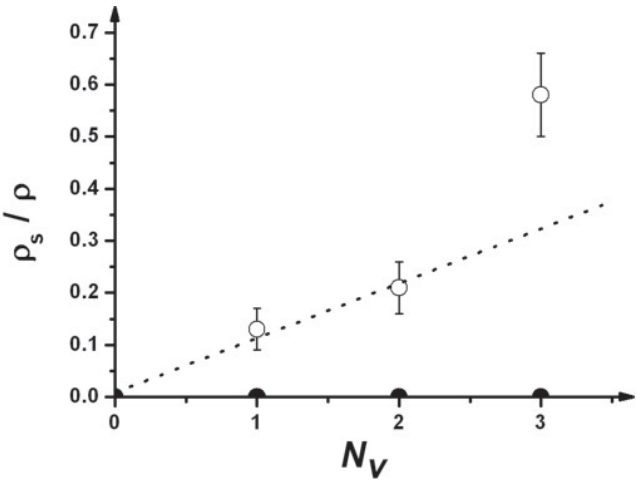


FIG. 4. Superfluid fraction of the $C_{1/3}$ commensurate solid of $^4$He atoms adsorbed on graphene versus the number of vacancies $N_v$. The computations were done at a temperature $T = 0.31$ K for a $9 \times 6$ rectangular simulation cell. The open circles are for the isotropic LJ potentials while the closed circles are for the anisotropic pair potentials.

properties of the $^4$He monolayer on a graphene critically depend on the substrate potential, especially at low helium coverages. With the anisotropic $^4$He-C pair potentials, which give the best fit to $^4$He scattering from graphite, we could find neither mobile vacancy states nor a supersolid phase in the helium monolayer on graphene even for the smaller $9 \times 6$ simulation cell.

We now discuss results of the monolayer on graphene at higher densities using the anisotropic LJ pair potential. Figure 5 shows the density distributions of $^4$He atoms at three different coverages for the $12 \times 8$ simulation cell. As seen in Fig. 5(a), a domain wall occurs at 0.0716 Å$^{-2}$ coverage, slightly higher than the 1/3 commensurate filling. The density distribution for a coverage of 0.0835 Å$^{-2}$ in Fig. 5(b) shows a $4 \times 4$ registered structure where seven $^4$He adatoms and 16 adsorption sites are included in a rhombic unit cell enclosed by yellow dashed lines. This 7/16 commensurate structure was identified in the $D_2$ monolayer on graphite from neutron diffraction and specific heat measurements.[25] For the $^4$He monolayer on graphite it was first observed in the PIMC calculations of Corboz *et al.*[9] They concluded that this state corresponds to the high-density commensurate solid which Greywall and Busch[3] predicted at a coverage of 0.0820 Å$^{-2}$, only about 2% lower than the 7/16 filling, from their heat capacity data for the $^4$He monolayer on graphite. We find that despite weaker binding of $^4$He atoms to graphene as opposed to graphite, the same commensurate structure can be realized. As expected, the $^4$He atoms constitute an incommensurate triangular solid at the highest density of $\sigma = 0.103$ Å$^{-2}$ considered here [see Fig. 5(c)]. We have found that the finite size of the simulation cell does not have much effect on the high-density phases of Fig. 5; at the coverage of 0.0835 Å$^{-2}$, both the peak position of the static structure factor and its peak value divided by the number of $^4$He atoms do not change for different system sizes with the latter being 0.0293(2), 0.0291(1), and 0.0287(2) for the $8 \times 8$, $12 \times 8$, and $16 \times 8$ simulation cell, respectively. According to our PIMC calculations the monolayer of $^4$He adatoms on a graphene surface exhibits similar quantum phase transitions at high helium coverages to those proposed for helium on graphite: it shows a commensurate structure at the 1/3 filling and goes through domain-wall phases at higher densities before crystallizing into an incommensurate triangular solid near its completion. An additional 7/16 commensurate structure emerges between the domain-wall regime and the incommensurate solid regime.

### B. The second layer

Since the torsional oscillator experiments of Crowell and Reppy first revealed finite superfluid fractions at helium coverages near those of a conjectured commensurate solid phase,[6] there have been speculations regarding the possibility of a two-dimensional supersolid phase in the second helium layer above graphite. Whether a stable commensurate structure with respect to a first-layer triangular solid does exist in the second $^4$He layer remains unresolved. Its existence is critical in determining whether a vacancy-based supersolid phase could be realized. In previous PIMC calculations for

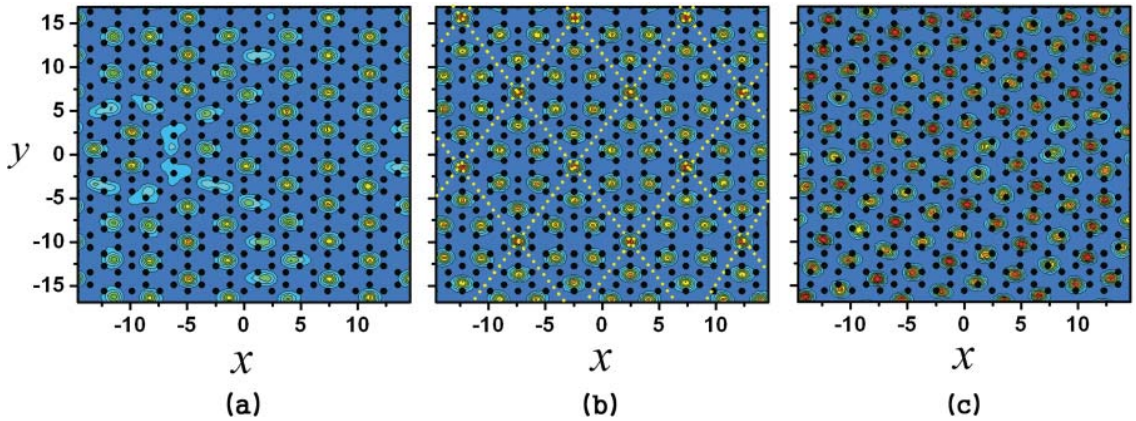


FIG. 5. (Color online) Densities of a single $^4$He monolayer on graphene at coverages of (a) 0.0716 Å$^{-2}$, (b) 0.0835 Å$^{-2}$, and (c) 0.103 Å$^{-2}$ using an anisotropic Lennard-Jones pair potentials in a $12 \times 8$ rectangular simulation cell with dimension $29.51 \times 34.08$ Å$^{-2}$. The black dots represent the locations of carbon atoms. The unit of length is Å.

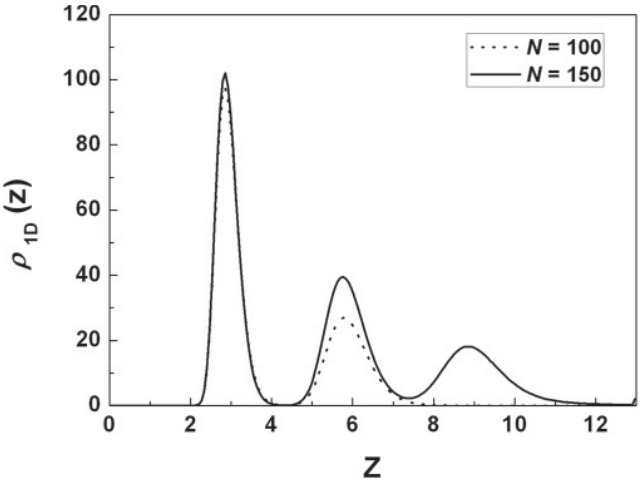


FIG. 6. One-dimensional density of $^4$He atoms above graphene as a function of the distance $z$ (in Å) from the graphene surface for 100 and 150 $^4$He atoms in a $9 \times 6$ rectangular simulation cell. The sum of the anisotropic Lennard-Jones pair potentials was used for the $^4$He-substrate interaction.

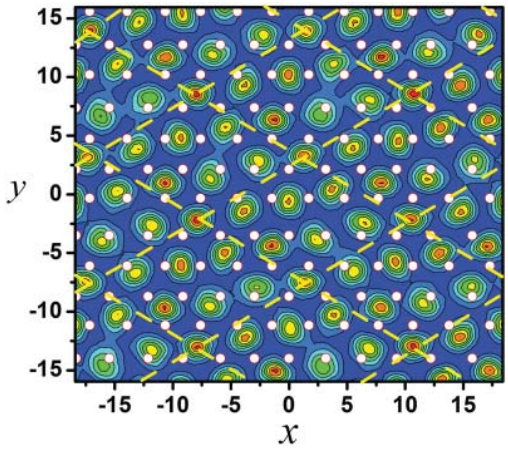


FIG. 7. (Color online) The two-dimensional density of the second-layer $^4$He atoms at a second-layer coverage of 0.07 Å$^{-2}$, which was computed at $T = 0.5$ K without particle exchanges. The small white circles represent the peak positions of the first-layer helium density whose coverage is 0.12 Å$^{-2}$. A rhombus enclosed by the yellow dotted lines shows a unit cell of the $C_{7/12}$ structure.

the second $^4$He layer on graphite, two different solid phases were discussed. Assuming a frozen first layer of $^4$He atoms (no zero-point motion), Pierce and Manousakis[7,8] observed a 4/7 commensurate structure in the second helium layer at coverage between a low-density liquid and a high-density incommensurate triangular solid. Stability of this $C_{4/7}$ structure, however, was not confirmed by Corboz *et al*.,[9] who found that a different commensurate structure, namely $C_{7/12}$ structure, was more stable than the $C_{4/7}$ structure. Furthermore, the $C_{7/12}$ structure was unstable when zero-point motions of the first-layer $^4$He atoms were incorporated. Since they could not find any stable commensurate structure, Corboz *et al*. concluded that a two-dimensional supersolid phase would not exist in the second helium layer on graphite.

We have also simulated the second $^4$He layer on a graphene. Figure 6 shows helium density distributions as a function of the distance $z$ from the graphene surface. They show distinct layered structures similar to those observed above graphite. The first density peak ($z \sim 2.8$ Å) gets sharper as more $^4$He atoms are adsorbed. This first-layer compression due to adsorption of successive helium layers was experimentally estimated to be as large as 6% on a graphite surface.[3,4] From one-dimensional density distribution for $N = 150$ in Fig. 6, we estimate the first-layer completion coverage to be $\sigma_1^{cl} = 0.12$ Å$^{-2}$. We note that from the analysis of heat capacity data, Greywall and Busch[3] proposed a value of 0.127 Å$^{-2}$ for the first-layer completion on graphite, about 6% higher than our estimated value for graphene. The second density peak in Fig. 6 occurs for values of $z$ (~5.8 Å), where the corrugation of the substrate potential is minimal (see Fig. 1). This enables us to use a laterally averaged one-dimensional substrate potential in our calculations for the second helium layer.

The stability of commensurate structures discussed in the previous PIMC studies for graphite surface is investigated here for the second layer on graphene. As Pierce and Manousakis found on graphite,[7,8] we observe a $C_{4/7}$ commensurate solid above a frozen first layer on a graphene. However, this structure is found to be unstable when the first-layer helium atoms are allowed to be dynamic along with the second-layer atoms. We also find that a 7/12 commensurate structure is more stable than the 4/7 structure on graphene. Figure 7 shows the second-layer density distribution at a coverage of 0.07 Å$^{-2}$. In this computation, which was performed at 0.5 K, all $^4$He atoms were dynamic but quantum exchanges among them were prohibited. The small white circles in Fig. 7 represent the peak positions of the first-layer density distribution. A rhombic unit cell, enclosed by yellow dotted lines in Fig. 7, includes 7 second-layer $^4$He atoms above 12 first-layer atoms. While it is stable without exchange coupling among the helium atoms, the triangular structure is found to be disrupted and eventually to disappear as a result of particle exchanges, most notably three-particle ring exchanges. This exchange-induced quantum melting is similar to the melting mechanism proposed for the vortex lattices in a rotating quasi-two-dimensional Bose-Einstein condensate.[26] While Corboz *et al*. concluded that the instability of the $C_{7/12}$ structure on graphite was due to the zero-point motions of the first-layer $^4$He atoms, we have found that quantum exchanges of $^4$He atoms are responsible for melting of the 7/12 structure on graphene. This leads us to a speculation that suppression of quantum exchanges with the addition of $^3$He impurities might stabilize a commensurate structure in the second helium layer on graphene. Unlike the corresponding $^4$He layer, the second layer of $^3$He atoms on graphite was reported to have a stable commensurate structure.[27] Some years ago, Kalos *et al*.[28] showed from Green's function Monte Carlo calculations that a quantum hard-sphere system solidifies at a lower density than its classical counterpart; this can be understood by the increase in effective hard sphere radii due to quantum fluctuations. From this one can argue that larger quantum fluctuations contribute to the stability of a $^3$He crystalline structure on graphite. However, our observation of exchange-induced melting of a $^4$He commensurate solid on graphene says that the stability

difference between the $^3$He layer and the $^4$He layer is mainly due to different quantum statistics of their constituents.

## IV. CONCLUSIONS

We have performed PIMC calculations for the first and the second layer of $^4$He atoms adsorbed on graphene. With the $^4$He-graphene interaction described by the sum of an isotropic $^4$He-C 6-12 pair potential, the first helium layer is found to be in a liquid state at helium coverages below the 1/3 commensurate filling and to exhibit vacancy-based supersolidity in the $C_{1/3}$ commensurate structure. These are consistent with recent zero-temperature DMC calculations of Gordillo *et al.*,[10,11] which were based on the same substrate potential. With the anisotropic $^4$He-C pair potentials, however, we find that the first layer is in a mixed state between a gas and the $C_{1/3}$ solid at low density and that a cluster of localized vacancy states are formed in the 1/3 commensurate solid without any contribution to superfluidity. This difference is due to the fact that the $^4$He-graphene potential based on the isotropic pair potentials greatly reduces its corrugation along the planar directions compared to the substrate potential based on the fully anisotropic pair potentials. A definitive conclusion of whether this helium layer will exhibit vacancy-based supersolidity would require a more accurate $^4$He-graphene potential. With anisotropic pair potentials, which provided the best fit to helium scattering from graphite,[12] we did not observe any supersolidity in the first helium layer.

The monolayer of $^4$He atoms on a single graphene sheet undergoes various domain-wall phases at higher areal densities than the 1/3 commensurate density and freezes into an incommensurate triangular solid near its completion. An additional 7/16 commensurate structure observed just before entering the incommensurate solid regime is believed to correspond to the high-density commensurate solid that Greywall and Busch[3] proposed for the $^4$He monolayer on graphite. We have observed exchange-induced melting of a 7/12 commensurate structure in the second $^4$He layer on graphene. We are currently investigating its stabilization through the suppression of particle exchanges by $^3$He impurities.

## ACKNOWLEDGMENTS

This work was supported by the Materials Computation Center funded by National Science Foundation Grant No. DMR03-25939 ITR and the Institute of Condensed Matter Theory at the University of Illinois and by the National Research Foundation of Korea funded by the Korean Government (Grants No. NRF-2010-013-C00014 and No. R31-2008-000-10057-0 to Y.K.).

[1] O. Leenaerts, B. Partoens, and F. M. Peeters, Appl. Phys. Lett. **93**, 193107 (2008).
[2] G. Zimmerli, G. Mistura, and M. H. W. Chan, Phys. Rev. Lett. **68**, 60 (1992).
[3] D. S. Greywall and P. A. Busch, Phys. Rev. Lett. **67**, 3535 (1991).
[4] D. S. Greywall, Phys. Rev. B **47**, 309 (1993).
[5] P. A. Crowell and J. D. Reppy, Phys. Rev. Lett. **70**, 3291 (1993).
[6] P. A. Crowell and J. D. Reppy, Phys. Rev. B **53**, 2701 (1996).
[7] M. E. Pierce and E. Manousakis, Phys. Rev. Lett. **81**, 156 (1998).
[8] M. E. Pierce and E. Manousakis, Phys. Rev. B **59**, 3802 (1999).
[9] P. Corboz, M. Boninsegni, L. Pollet, and M. Troyer, Phys. Rev. B **78**, 245414 (2008).
[10] M. C. Gordillo and J. Boronat, Phys. Rev. Lett. **102**, 085303 (2009).
[11] M. C. Gordillo, C. Cazorla, and J. Boronat, Phys. Rev. B **83**, 121406(R) (2011).
[12] W. E. Carlos and M. W. Cole, Surf. Sci. **91**, 339 (1980).
[13] M. E. Pierce and E. Manousakis, Phys. Rev. Lett. **83**, 5314 (1999).
[14] G. Stan and M. W. Cole, Surf. Sci. **395**, 280 (1998).
[15] M. W. Cole, V. H. Crespi, G. Stan, C. Ebner, J. M. Hartman, S. Moroni, and M. Boninsegni, Phys. Rev. Lett. **84**, 3883 (2000).
[16] M. C. Gordillo, Phys. Rev. Lett. **101**, 046102 (2008).
[17] E. S. Hernandez, M. W. Cole, and M. Boninsegni, Phys. Rev. B **68**, 125418 (2003).
[18] Y. Kwon and H. Shin, Phys. Rev. B **82**, 172506 (2010).
[19] H. Shin and Y. Kwon, J. Chem. Phys. **136**, 064514 (2012).
[20] L. W. Bruch, M. W. Cole, and H.-Y. Kim, J. Phys.: Condens. Matter **22**, 304001 (2010).
[21] D. M. Ceperley, Rev. Mod. Phys. **67**, 279 (1995).
[22] R. A. Aziz, M. J. Slaman, A. Koide, A. R. Allnatt, and W. J. Meath, Mol. Phys. **77**, 321 (1992).
[23] R. E. Zillich, F. Paesani, Y. Kwon, and K. B. Whaley, J. Chem. Phys. **123**, 114301 (2005).
[24] We could not compute the superfluid fractions for the bigger 12 × 8 system because of an ergodicity problem of our permutation sampling, which was discussed in detail in Ref. 21.
[25] H. Freimuth, H. Wiechert, H. P. Schildberg, and H. J. Lauter, Phys. Rev. B **42**, 587 (1990).
[26] T. K. Ghosh and G. Baskaran, Phys. Rev. A **69**, 023603 (2004).
[27] H. Fukuyama, J. Phys. Soc. Jpn. **77**, 111013 (2008).
[28] M. H. Kalos, D. Levesque, and L. Verlet, Phys. Rev. A **9**, 2178 (1974).